Geochemistry Geophysics Geosystems G3

Article
Volume 11, Number 12
24 December 2010
Q12010, doi:10.1029/2010GC003305
ISSN: 1525-2027

Published by AGU and the Geochemical Society

Rapid, continuous streaking of tremor in Cascadia

Abhijit Ghosh, John E. Vidale, Justin R. Sweet, Kenneth C. Creager, Aaron G. Wech, and Heidi Houston

Department of Earth and Space Sciences, University of Washington, Seattle, Washington 98195, USA (aghosh.earth@gmail.com)

Emily E. Brodsky

Department of Earth and Planetary Sciences, University of California, Santa Cruz, California 95064, USA

[1] Nonvolcanic tremor is a recently discovered weak seismic signal associated with slow slip on a fault plane and has potential to answer many questions about how faults move. Its spatiotemporal distribution, however, is complex and varies over different time scales, and the causal physical mechanisms remain unclear. Here we use a beam backprojection method to show rapid, continuous, slip-parallel streaking of tremor over time scales of several minutes to an hour during the May 2008 episodic tremor and slip event in the Cascadia subduction zone. The streaks propagate across distances up to 65 km, primarily parallel to the slip direction of the subduction zone, both updip and downdip at velocities ranging from 30 to 200 km/h. We explore mainly two models that may explain such continuous tremor streaking. The first involves interaction of slowly migrating creep front with slip-parallel linear structures on the fault. The second is pressure-driven fluid flow through structurally controlled conduits on the fault. Both can be consistent with the observed propagation velocities and geometries, although the second one requires unlikely condition. In addition, we put this new observation in the context of the overall variability of tremor behavior observed over different time scales.

Components: 5400 words, 9 figures, 1 animation.

Keywords: nonvolcanic tremor; tremor streak; spatiotemporal distribution; migration; fluid flow; Cascadia subduction zone.

Index Terms: 7230 Seismology: Seismicity and tectonics (1207, 1217, 1240, 1242); 8104 Tectonophysics: Continental margins: convergent; 8045 Structural Geology: Role of fluids.

Received 23 July 2010; **Revised** 12 October 2010; **Accepted** 18 October 2010; **Published** 24 December 2010.

Ghosh, A., J. E. Vidale, J. R. Sweet, K. C. Creager, A. G. Wech, H. Houston, and E. E. Brodsky (2010), Rapid, continuous streaking of tremor in Cascadia, *Geochem. Geophys. Geosyst.*, *11*, Q12010, doi:10.1029/2010GC003305.

1. Introduction

[2] Episodic tremor and slip (ETS) in the Cascadia subduction zone (CSZ) provides an excellent opportunity to study the transition zone seismicity that takes the form of nonvolcanic tremor (NVT). Slow slip events may contribute to seismic hazard analyses, as they occur downdip of the locked part of the subduction fault, which produces large and destructive earthquakes. Geodetic observations during slow slip episodes delineate slipping patches on the plate boundary smoothed over several days in time, and several tens of kilometers in space. But recent high-resolution observations from a dense seismic array indicate a more complex evolution of NVT (and therefore ETS) spanning over a broad range of time and length scales [*Ghosh et al.*, 2009a; *Ghosh et al.*, 2010]. Hence, understanding styles of NVT propa-

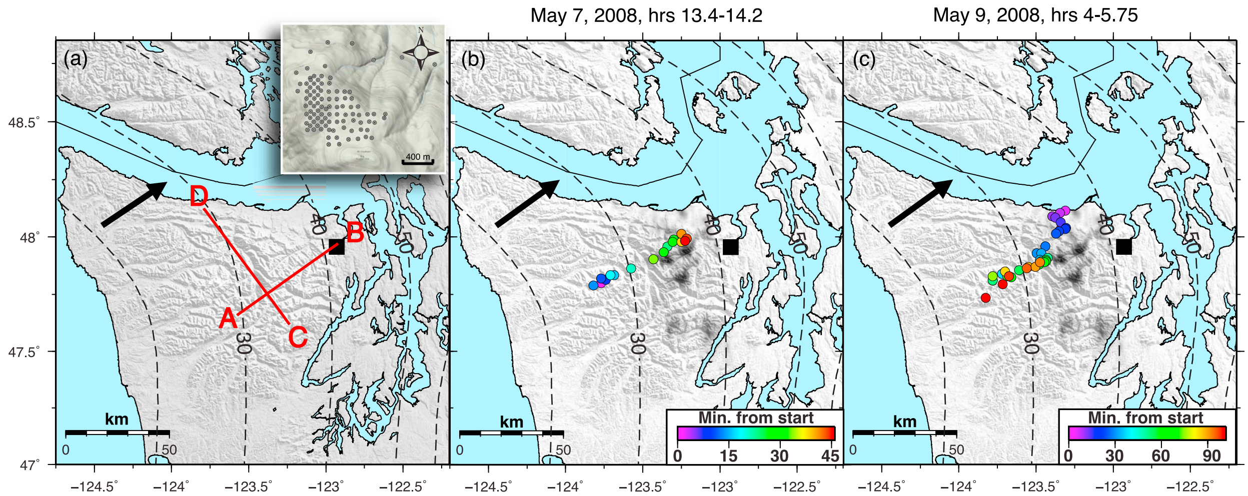

Figure 1. Location map and tremor streaks: colored circles in the maps represent tremor locations using the beam backprojection method [*Ghosh et al.*, 2009a]. Time is color coded to show tremor migration. Black solid square marks the Big Skidder array. Arrows indicate overall slip direction of CSZ. Dashed contour lines shows plate interface depth in km. Gray patches in Figures 1b and 1c show tremor moment patches [*Ghosh et al.*, 2009a]; the darker the patch, the higher the moment release. (a) Location map of the study area. Lines AB and CD are oriented parallel and perpendicular to the slip direction, respectively, and are used to generate Figure 3. Inset shows the station distribution of the Big Skidder array. (b) Slip-parallel tremor streak showing rapid downdip short-term migration of tremor with a horizontal velocity of 60 km/h. (c) Slip-parallel tremor streak rapidly propagating updip with a horizontal velocity of 35 km/h.

gation across a range of length and time scales may give new insight into the tremor mechanism, and help clarify the physics of slow slip events.

[3] The broad region of tremor activity is well mapped by envelope cross correlation (ECC) methods [e.g., *Nadeau and Dolenc*, 2005; *Obara*, 2002; *Wech and Creager*, 2008]. But the spatial resolution of ECC methods does not resolve fine-scale spatiotemporal details of NVT evolution. Different patterns of tremor migration possibly indicate complex interactions of various processes that govern the subduction boundary system. Interestingly, it appears that tremor behavior markedly varies over the time scales of observation. Over time scales of several days, tremor activity releases moment from several distinct patches [*Ghosh et al.*, 2009a]. Over time scales of several hours, slip-parallel bands of tremor activity migrate along strike with a velocity of ~10 km/d [*Ghosh et al.*, 2010]. Over the time scale of several minutes, low-frequency earthquake (LFE) activity suggests sporadic faster tremor migration in the western Shikoku, Japan subduction zone [*Shelly et al.*, 2007a], and beneath the San Andreas Fault, near Parkfield [*Shelly*, 2009]. How these different NVT behaviors are linked to produce the overall large-scale ETS activity is poorly understood.

[4] Here we show rapid, continuous, slip-parallel faster tremor migration that produces streaks of tremor within an ETS event in Cascadia, and explore the physics of two simple models for generating such tremor migration over the time scale of several minutes to an hour. In addition, we combine different elements of spatiotemporal tremor distribution (i.e., tremor streaks, bands, and moment patches), illustrate their relationship with each other, and the slow slip event, and provide a more complete picture of tremor distribution in space and time.

2. Data and Method

[5] We use seismic recordings of the May 2008 ETS event in northern CSZ by an 84-element, small-aperture, vertical component seismic array, henceforth, the Big Skidder array. It was installed on the Olympic Peninsula, Washington, USA, above the migration path of this ETS event [*Ghosh et al.*, 2009a] (Figure 1). We use a beam backprojection (BBP) method [*Ghosh et al.*, 2009a] to detect and locate tremor. The BBP method applied here stacks and beamforms 3–8 Hz seismic energy using 5 min sliding time windows with 50% overlap. Tremor is detected and located from the beamformer output assuming that NVT is occurring at the plate interface. There is a growing consensus that tremor occurs at the plate interface as a result of shear slip on the fault plane [*Brown et al.*, 2009; *Ghosh et al.*,

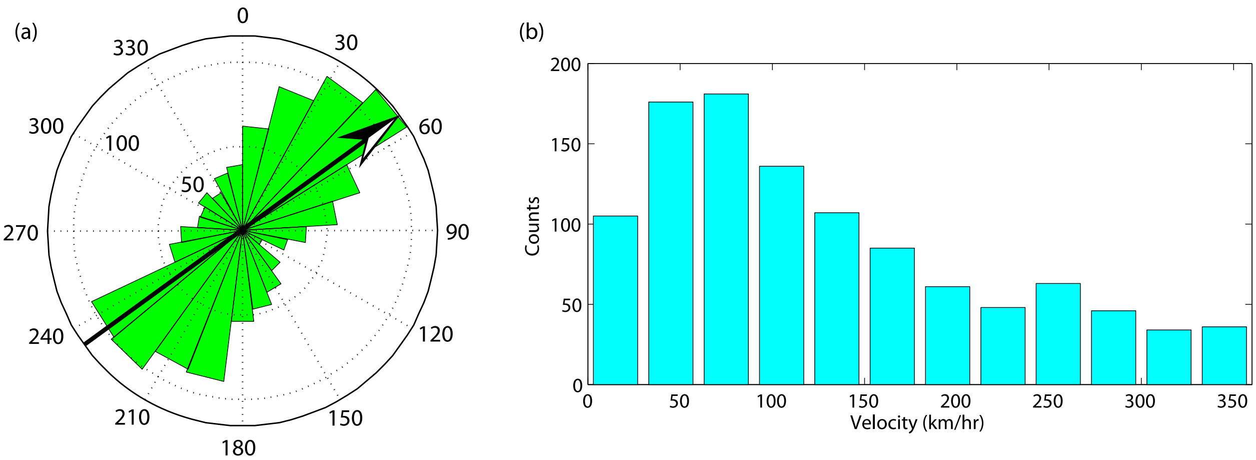

Figure 2. (a) Rose diagram showing dominant direction of continuous, rapid tremor migration is parallel to the overall slip direction of CSZ (arrow). Peripheral numbers are propagation azimuths in degrees, and radial numbers are counts of tremor windows. (b) Histogram of tremor velocity between adjacent time windows. The diagrams are constructed using all the tremor locations for 6 and 7 May 2008, when tremor was strong and virtually continuous under the Big Skidder array. Two-minute time windows are used to get good statistics. Independent windows are used to avoid any possible artifacts due to time overlap. Propagation direction and velocity are calculated between two adjacent tremor time windows.

2009b; *La Rocca et al.*, 2009; *Rubinstein et al.*, 2007; *Shelly et al.*, 2006, 2007b, 2009], although a complete unanimity is yet to be reached [*Kao et al.*, 2005]. The BBP method can detect up to four times more tremor than the ECC method during the period of weak tremor activity [*Ghosh et al.*, 2009a], gives high resolution in relative tremor location, and thus tracks tremor in space and time in great detail. The configuration of the Big Skidder array, the BBP method, and the validity of the assumptions are discussed at length by *Ghosh et al.* [2009a].

3. Observations: Tremor Streaks

[6] We track NVT activity continuously during the May 2008 ETS event in northern CSZ using the BBP method to reveal some hitherto unseen features of tremor migration in Cascadia. Over the time scale of several minutes to an hour or so, tremor propagates rapidly, and near-continuously (please see Animation 1)[1] with horizontal velocities ranging from 30 to 200 km/h. This is in contrast to the ECC tremor locations during the same time period that show flickering NVT activity jumping randomly within a larger tremor-active region. While we observe nearly continuous rapid streaking of tremor using the BBP method in Cascadia, rapid tremor propagation observed using LFE method in western Shikoku, Japan, appears to be sporadic [*Shelly et al.*, 2007a]. This discrepancy could be caused by the limited number of identifiable LFE templates used so far to locate tremor in Japan.

[7] Over a 2 min time scale, tremor usually migrates either updip or downdip parallel to the overall slip direction of the CSZ (Figure 2a). Occasionally, tremor also migrates rapidly along strike, or persists in a small area. A histogram of tremor migration velocity between two consecutive locations using independent 2 min time windows reveals dominant velocities of 30–90 km/h (Figure 2b). The tail of the histogram is difficult to interpret as it possibly contains significant contribution from tremor jumps, e.g., jumps from the end of a streak to the start of another or two tremor sources significantly separated in space but active simultaneously. Short-term tremor migration shows a streaky nature in general, with varied degree of continuity (Figure 3). Similar analysis over 5 min time scale produces the same general features.

[8] A number of conspicuous tremor streaks are identified by visual inspections, and cataloged for further analyses. We define streaks as the rapid tremor migration that shows reasonable continuity in space and time, lasts at least 10 min, and propagates more than 10 km horizontally. Using these criteria, we are able to identify 27 streaks (Table S1) that are recorded by our short-lived Big Skidder array.[2] Examples of two such distinct tremor streaks are shown in Figures 1b and 1c. Over short time

[1]Animations are available in the HTML.

[2]Auxiliary materials are available in the HTML. doi:10.1029/2010GC003305.

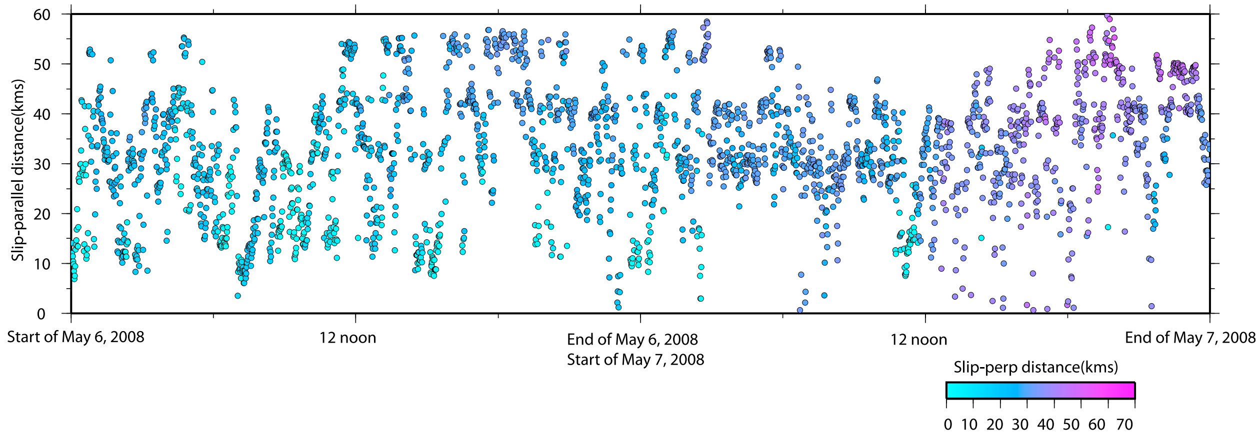

Figure 3. Tremor distribution in space-time domain. Colored circles represent tremor locations using the beam back-projection method. The *x* and *y* axes represent time and distance along line AB in Figure 1a, respectively. Distance increases from A to B. Distance along line CD in Figure 1a is color coded. Distance increases from C to D. Note the overall streaky nature of short-term tremor migration.

scales, individual streaks can show a complex migration pattern, as opposed to a perfectly constant velocity from start to finish. They often change velocity, propagate back and forth, and even change the direction of propagation (Figures 1b and 1c), although we do not find any systematic variation. Collectively, the majority of the catalog consists of unilaterally propagating slip-parallel streaks (21 out of 27, Figure 4a), which are also the longest, and the most prominent ones. The majority of the streaks propagate at velocities ranging between 30 and 110 km/h, with a peak around 70 km/h (Figure 4b). The directional rose diagram (Figure 4a), and the velocity histogram (Figure 4b) generated from the streak catalog are essentially a crude reflection of similar analysis done with the consecutive tremor locations with 2 min independent time windows (Figure 2), suggesting that the streak catalog is able to capture the main features of short-term tremor migration reasonably well. About 80% of the tremor streaks lasted less than half an hour, but we do observe streaks that continue propagating for nearly 2 h (Figure 4d). A histogram of the lengths of the streaks shows a broad peak, with about 85% being

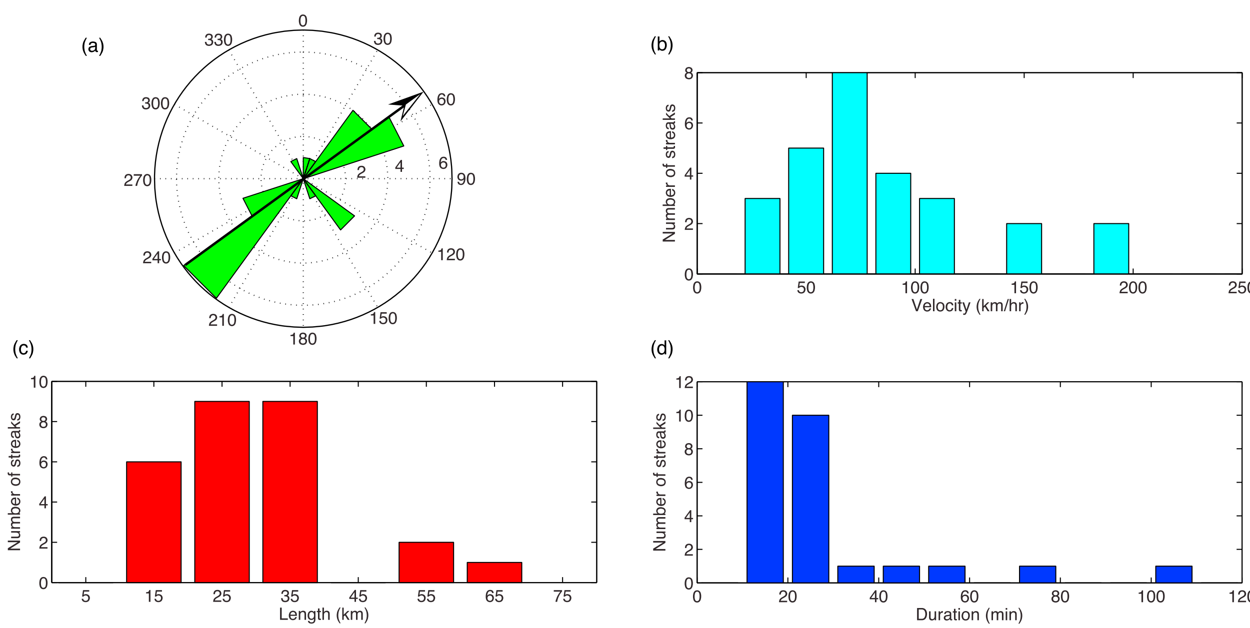

Figure 4. Statistics of the tremor streaks identified and cataloged. Twenty-seven tremor streaks are used to generate the statistics. (a) Rose diagram showing the direction of propagation. Peripheral numbers are propagation azimuths in degrees, and radial numbers are counts of tremor streaks. Histograms of the (b) velocity, (c) length, and (d) duration.

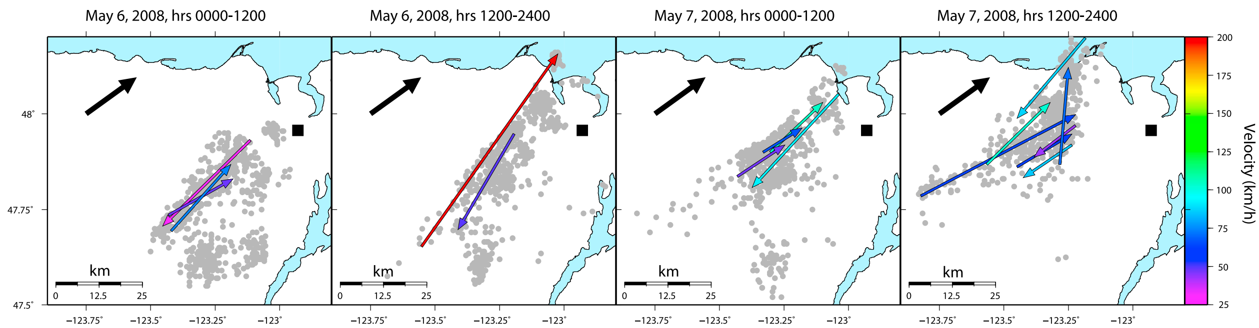

Figure 5. Each of the four panels shows 12 h of tremor locations (gray solid circles) using beam backprojection method. Colored arrows indicate velocity and direction of rapid tremor streaking during each time segment. Velocity is color coded. Note that slip-parallel tremor streaking activity moves along strike with slip-parallel tremor bands [*Ghosh et al.*, 2010]. Bold black arrow indicates the slip direction of CSZ, and black square marks Big Skidder array.

less than 40 km (Figure 4c). Occasionally, tremor propagates rapidly for more than 50 km.

[9] Slip-parallel streaking is interesting considering that the tremor bands associated with the long-term, along-strike, slower tremor migration also align themselves parallel to the overall slip direction in this part of the subduction zone [*Ghosh et al.*, 2010]. Moreover, slip-parallel streaking tremor slowly migrates along strike south to north coinciding with the shifting tremor bands (Figure 5). The tremor streaks often light up the tremor moment patches [*Ghosh et al.*, 2009a] by a combination of increased relative moment release, and longer residence time within the patches. In addition, the streaks tend to propagate along the same track multiple times. Figure 6 shows an example of such repeating propagation tracks, along which tremor streaks propagate at least 3 times in less than 1 h.

4. Exploring Possible Mechanisms of Streak Propagation

[10] While the observations are clear and intriguing, unraveling the driving mechanism behind continuous tremor streaking is challenging; especially given that the tremor activity shows remarkable variability in velocities over different time scales. In addition, the strikingly slip-parallel tremor migration, and repeating propagation tracks of streaking tremor suggest a strong control of geologic structure over tremor propagation track. Over longer time scales, along-strike migration of slip-parallel tremor bands with a velocity of ~10 km/d

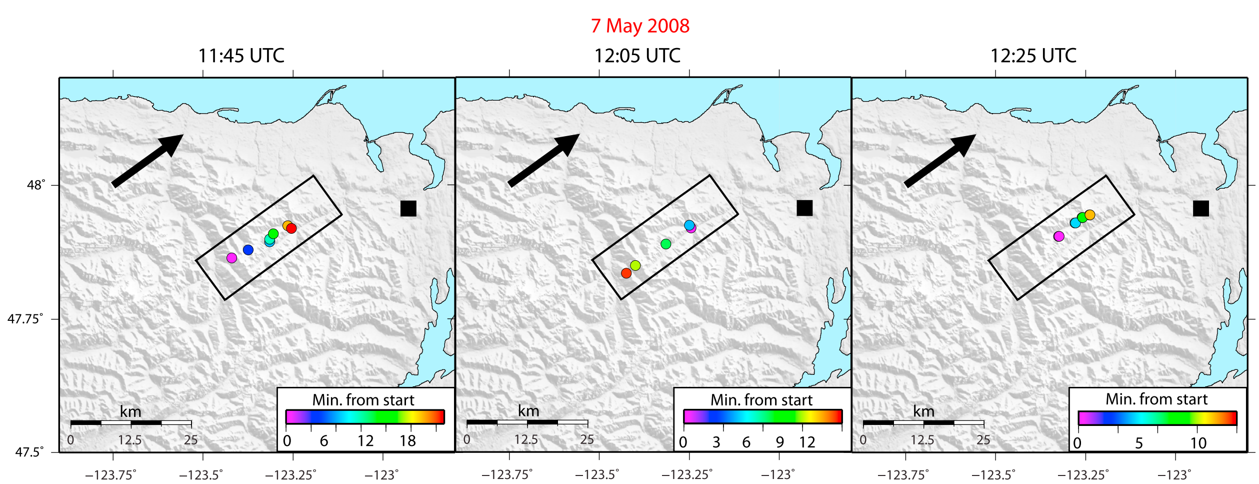

Figure 6. Tremor streaks repeat the same track multiple times: colored circles represent tremor locations using the beam backprojection method. Time is color coded to show tremor migration. Black solid square marks the Big Skidder array. Arrow indicates overall slip direction of CSZ. Black rectangle with the long axis parallel to the slip direction is for reference. The time above each map indicates the start of the tremor propagation. Note that tremor streaks repeat similar tracks three times in less than 1 h.

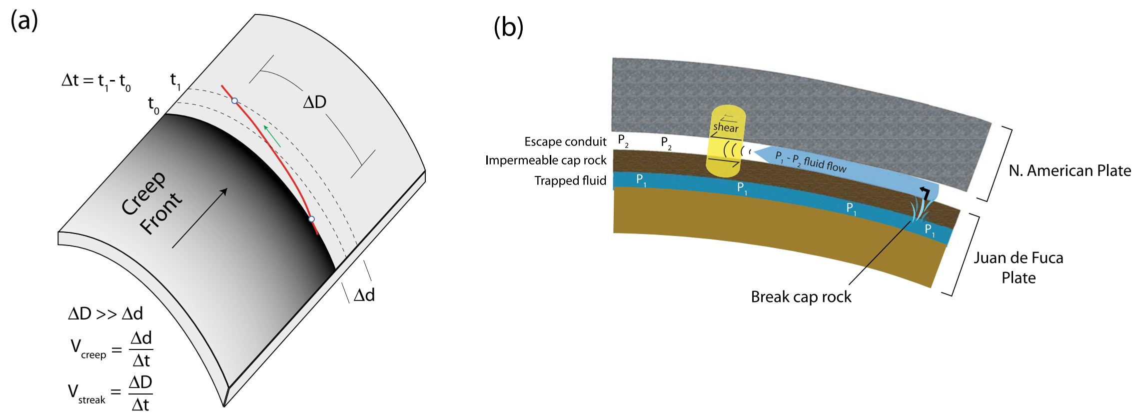

Figure 7. (a) Schematic diagram showing the interaction between the creep front and slip-parallel linear structure to produce tremor streak. Gray shading represents the creep front that moves slowly (~10 km/d) along strike, which is associated with long-term tremor migration. Dashed lines show the leading edge of the creep front migrating with time. The red line marks linear slip-parallel structure on the fault, which makes a small angle with the leading edge of the creep front. As the creep front slowly moves in the direction of the black arrow, it generates tremor along the red line (linear structure) producing rapidly propagating tremor streak. The green arrow marks the streak propagation direction. (b) Schematic diagram depicting fluid flow-induced shear slip causing streaking tremor: pressure-driven fluid flow through a conduit. The diagram shows a small region in the ETS zone with near-lithostatic fluid pressure (P_1) beneath the caprock (plate interface). Fluid pressure is hydrostatic (P_2) everywhere just above the interface. When thin caprock at the interface breaks, the pressure difference along the interface (escape conduit) is $P_1 - P_2 = 0.63$ GPa. Fluid flow through the conduit is driven by this pressure difference. As fluid flows through the conduit, it perturbs the stress field and triggers shear failure.

has been attributed to progressive slow slip and resulting stress transfer on the fault plane [*Ghosh et al.*, 2010]. Invoking a similar stress transfer mechanism for rapid tremor migration over short time scale (tremor streak) might be appealing. For instance, each tremor event in a streaking sequence could be the result of stress induced by its preceding events [*Shelly et al.*, 2007a]. Although simple, this model, however, cannot decipher an important piece of the puzzle: why does stress transfer act at different velocities over different time scales, all much slower than the elastic waves? Here we explore different alternative models that might be able to produce continuous, rapid tremor streaking over short time scales during an ETS event.

[11] In unraveling this puzzle, it is important to note that the slip, and dip direction of the plate interface model differ by up to 35° in this region. It has long been known that fault surface exposures show prominent linear striations, corrugations/mullions [*Smith*, 1975, 1977], and ridge-and-groove structures with their long-axis parallel to the slip direction [*Power and Tullis*, 1992; *Resor and Meer*, 2009; *Rubin et al.*, 1999; *Sagy et al.*, 2007]. One possibility is that tremor propagates along these slip-parallel, linear features on the fault plane to produce the observed continuous slip-parallel streaking activity. We propose a scenario with heterogeneity similar to *Ando et al.* [2010], in which the rheological and geometric distinction of the corrugations/ridges preferentially gives rise to rapidly propagating slip-parallel tremor streaks as the creep front sweeps across the ridges (Figure 7a).

[12] To evaluate the scenario, we calculate the geometrical constraints required for the corrugation/ridges to explain the propagation velocity of tremor streaks. The long-term migration can result from a creep front slowly migrating along strike with its leading edge approximately parallel to the slip direction [*Ghosh et al.*, 2010]. If tremor streaks mostly occur along the linear slip-parallel structures on the fault plane, a small difference in the angles between the linear structures and the migrating creep front will produce tremor streaks that propagate rapidly in approximately the slip-parallel direction. The relationship between the angle, and migration velocities is given by:

$$\theta = \sin^{-1}\left(\frac{V_L}{V_S}\right)$$

where θ is the angle between the linear structures and the migrating creep front, V_L is the long-term (creep front) velocity, and V_S is the short-term (streak) velocity. Indeed, ~0.5° difference in the angle can produce a streak propagating at ~50 km/h, the typical propagation velocity of the tremor streaks. This model is based on the geometrical features of the plate interface, and does a good job of connecting slower long-term and faster short-term tremor migrations with essentially the same driving mechanism, but does not address the occasional short-term faster along-strike migration that has been seen both in CSZ, and western Shikoku, Japan.

[13] A different approach can be taken by considering the possibility that the two very different natures and velocities of tremor migration may be a result of different driving mechanisms. We consider fluid migration through a conduit as a mechanism to generate rapidly propagating tremor streaks. Periodic breaking of impermeable caprock, and the resulting fluid release at the subduction interface has been suggested as an explanation to the periodic nature of ETS events [*Audet et al.*, 2009]. In this model, during an ETS event, fluid breaks the thin caprock at the interface when the pressure is sufficiently high, releasing high-pressure fluid at the interface. This creates the pressure gradient along the interface, as pore pressure is still hydrostatic just above the caprock (i.e., the plate interface). The released fluid finds the easiest way to flow, and gushes through the conduit made available by striations and grooves on the fault plane. As fluid flows through the conduits along the interface, it exerts pressure on the conduit wall. As a result, it perturbs effective normal stress, and may trigger shear failure on the interface, producing the observed rapidly propagating tremor (Figure 7b). This model has the potential to explain the propagation velocity of tremor streaks, and is consistent with the inferred presence of high fluid pressure near tremor-active region [*Audet et al.*, 2009; *Hyndman and Peacock*, 2003; *Peacock*, 2009; *Shelly et al.*, 2006].

[14] We now calculate the conditions required to move fluids at the observed migration speed. Fluids move very slowly by diffusion, but pressure-driven fluid flow through structurally controlled conduits is much faster. Near-lithostatic pore pressure just beneath the plate interface near the ETS zone has been inferred from slow shear wave speeds [*Audet et al.*, 2009; *Shelly et al.*, 2006]. Hence, the estimated pressure difference across the plate interface would be, assuming hydrostatic pressure above the interface:

$$(\rho_{crust} - \rho_{water})gh = 0.63 \text{ GPa}$$

where ρ_{crust} is the density of the crust (2800 kg/m^3), ρ_{water} is the density of the water (1000 kg/m^3), g is the acceleration due to gravity (10 m/s^2), and h is depth below the surface (35 km). The high Reynolds number indicates a turbulent flow regime in this case. Turbulent flow of a Newtonian fluid, like water, flowing through a pipe is governed by the following equation [*Turcotte and Schubert*, 2002]:

$$\overline{u} = \left(\frac{4 \times 2^{1/4}}{0.3164}\right)^{4/7} \left(-\frac{1}{\rho}\frac{dp}{dx}\right)^{4/7} R^{5/7} \left(\frac{\rho}{\mu}\right)^{1/7}$$

where $\overline{u}$ is mean fluid velocity, ρ is density of the fluid, dp is the pressure difference across the length of the pipe, dx is the length of the pipe, R is the radius of the pipe, and μ is the dynamic viscosity of the fluid. Modeling of a Newtonian viscous fluid (water) with dynamic viscosity (μ) of 10^{-4} Pa s and water density (ρ) of 1000 kg/m^3 flowing through a 25 km long conduit with 0.63 GPa pressure drop across its length requires a conduit of radius 1.4 cm to produce flow velocity on the order of 50 km/h, as typically observed for the rapid, short-term tremor migration.

[15] The least constrained parameter in this model is the radius of the conduits. The dominant slip-parallel direction for rapid tremor migration is possibly guided by slip-parallel linear structures developed on the fault interface. Although, we used 25 km as a typical value for the length of tremor streaks in our model, we do occasionally observe streaks that propagate more than 50 km. For example, Figure 1c shows a tremor streak propagating 60 km in the slip parallel direction. In this particular case, we need a conduit with a radius of 1.6 cm, which is not much different from what we get using the typical values. According to our model, it is possible to move fluid through a conduit as long as 60 km, if sufficient high-pressure fluid exists in the system. Studies of crustal faults that witnessed slip up to 1 km show meter-scale elevation difference in the fault surface topography (ridge-and-groove structure) [e.g., *Sagy et al.*, 2007]. Hence, it is conceivable that a subduction fault at a depth of 35 km with thousands of kilometers slip has linear slip-parallel corrugations with centimeter-scale fault surface topography. We also observe tremor streaks repeating the same track multiple times. Tracks/conduits that are particularly favorable for streaking, combined with locally persistent zone of high fluid pressure may produce repeating streaks.

[16] This fluid flow model requires long pathways/conduits (up to 65 km long streak is observed in this study) for rapidly flowing fluids. Such long, continuous conduits/fractures in the tremor-active

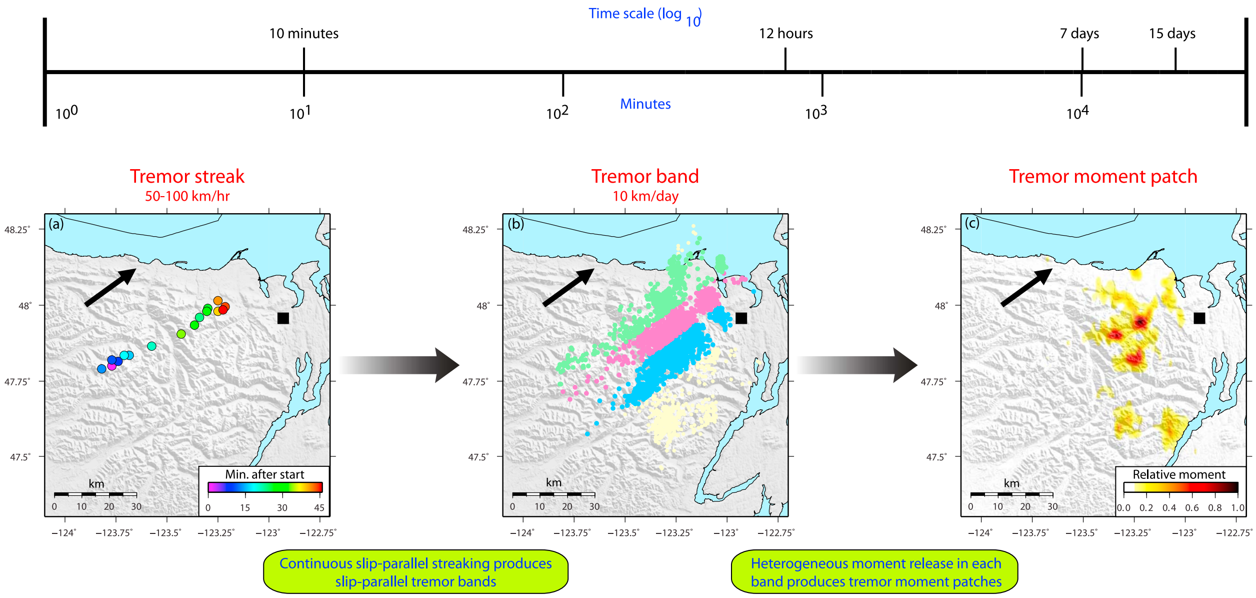

Figure 8. A unified view of tremor distribution in time and space: a time scale ($\log_{10}$) is shown at the top; time increases left to right. The maps show different elements of spatiotemporal tremor distribution observed over different time scales. Positions of the maps along the time scale approximately correspond to the time scales over which these elements are typically observed. Arrow in each map indicates slip direction of CSZ. Black solid square marks the Big Skidder array. (a) Slip-parallel tremor streak. Colored circles represent tremor locations. Time is color coded to show rapid tremor migration over short time scale. (b) Slip-parallel tremor bands defining the long-term slower (~10 km/d) along-strike tremor migration over time scales of hours to a day. Solid colored circles are tremor locations. Blue, pink, and green locations define the tremor bands [*Ghosh et al.*, 2010]. Faint yellow locations fall outside the tremor bands. Continuous slip-parallel streaking of tremor produces the tremor bands. (c) Relative band-limited tremor moment patches that release much of the seismic moment during an ETS event [*Ghosh et al.*, 2009a]. Uneven moment release within each band produces tremor patches.

region, however, seems unlikely. Perhaps networks of conduits/fractures are involved, and propagation of pressure pulses rather than fluid flow controls tremor migration. Investigating such complications are beyond the scope of this article. Nevertheless, although crude, the fluid flow model presented here would reconcile the different styles and velocities of tremor migration over different time scales. In addition, the occasional along-strike streaks could be explained by similar rapid fluid flow through isolated fractures aligned along-strike, possibly created at the outer rise. Models based on rate-and-state friction law (A. Rubin, Designer friction laws for bimodal slow slip propagation speeds, submitted to *Geochemistry, Geophysics, Geosystems*, 2010), dilatancy [*Segall and Bradley*, 2009], and migrating fluid pulse could perhaps accommodate the observations of rapidly propagating tremor streaks, and provide still more valuable alternatives.

5. Combining Spatiotemporal Scales

[17] Near-continuous streaking tremor, and the observations of tremor bands, and patches in Cascadia provide us with a unique opportunity to paint a more complete picture of the spatiotemporal distribution of tremor during an ETS event in Cascadia (Figure 8). Here we combine the observations of spatiotemporal tremor distribution made in our previous studies [*Ghosh et al.*, 2009a, 2010] with the tremor streaks presented in this article, discuss their relationship, and put them together in the context of the overall variability of tremor behavior observed over different time scales.

[18] Tremor distribution varies remarkably over different time scales. Over time scales of several minutes to an hour or so, tremor appears as near-continuously propagating streaks, which is associated with the short-term tremor migration, and seems to be the fundamental element of tremor distribution in space and time. In this case, tremor migrates rapidly (velocity ~30–200 km/h), and follows slip-parallel, possibly structurally controlled tracks on the fault interface. On the other hand, over time scales of several hours to a day, tremor activity organizes itself as elongated slip-parallel bands [*Ghosh et al.*, 2010]. These tremor

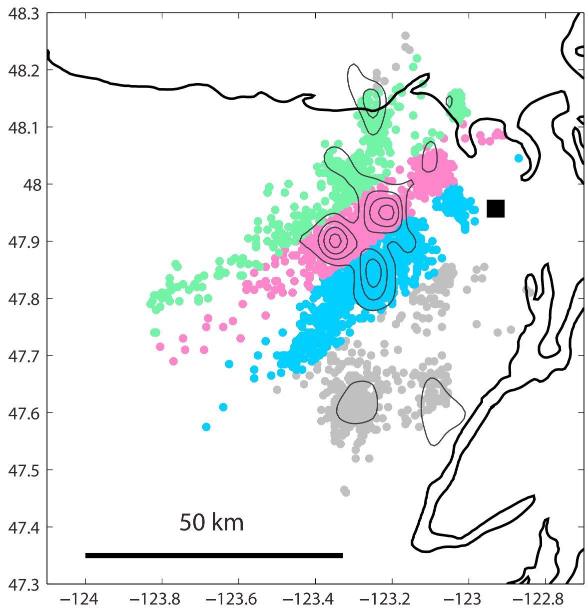

Figure 9. Blue, pink, and green solid circles are tremor locations that define three tremor bands [*Ghosh et al.*, 2010]. Gray locations fall outside the tremor bands. Contour lines show band-limited tremor moment patches [*Ghosh et al.*, 2009a]. Note that blue and pink tremor bands tightly contain three most prominent tremor moment patches. Black square marks Big Skidder array.

bands sweep Cascadia along-strike from south to north at a velocity of ~10 km/d, constituting long-term tremor migration. Tremor bands may illuminate slowly slipping strips on the plate interface. The resulting progressive along-strike transfer of stress may be responsible for long-term tremor migration. Along-strike shifting of streaking tremor activity with tremor bands (Figure 5), and their common slip-parallel alignment denote a close relationship between these two elements associated with short- and long-term tremor migrations. It suggests that slip-parallel tremor bands may be composed of multiple rapidly propagating slip-parallel tremor streaks. On the other hand, the uneven moment release within each tremor band (Figure 9) produces tremor moment patches that release much of the tremor moment during an ETS event, and are observed over time scale of several days to weeks. Moment patches may represent a heterogeneous plate interface with patches of low frictional coefficient and/or wet spots [*Ghosh et al.*, 2009a].

[19] More recently, rapid reversals of tremor (RTRs) have been observed during several ETS events in Cascadia (H. Houston et al., Rapid tremor reversals in Cascadia generated by slip on a weakened plate interface, submitted to *Nature Geoscience*, 2010). They propagate at an average velocity of 10 km/h, which is slower than the tremor streak, but faster than the tremor bands. In the range of time scales presented here (Figure 8), they typically fall between the tremor streaks and bands.

6. Summary and Conclusions

[20] We show continuous, slip-parallel tremor migration over short time scales (~1 h), producing rapidly propagating (~50 km/h) tremor streaks during an ETS event in Cascadia. We explored possible models that may explain such rapid, continuous streaking of tremor: interaction of slip-parallel corrugation with a migrating creep front, and fluid flow through slip-parallel conduits. By combining these different elements of spatiotemporal tremor distribution (i.e., tremor moment patches, bands, and streaks) observed over different time scales, we are able to present a more complete picture of tremor distribution in space and time. It may eventually lead toward a unified view of spatiotemporal tremor distribution as new elements are discovered, and added to this picture.

Acknowledgments

[21] We thank the Editor, Thorsten Becker, and two anonymous reviewers for their comments and suggestions. Thanks to Steve Malone and many volunteers for helping in the fieldwork and data management. Figures 1, 3, 5, 6, and 8 were created using Generic Mapping Tools [*Wessel and Smith*, 1998].

References

Ando, R., R. Nakata, and T. Hori (2010), A slip pulse model with fault heterogeneity for low-frequency earthquakes and tremor along plate interfaces, *Geophys. Res. Lett.*, *37*, L10310, doi:10.1029/2010GL043056.

Audet, P., M. G. Bostock, N. I. Christensen, and S. M. Peacock (2009), Seismic evidence for overpressured subducted oceanic crust and megathrust fault sealing, *Nature*, *457*(7225), 76–78, doi:10.1038/nature07650.

Brown, J. R., G. C. Beroza, S. Ide, K. Ohta, D. R. Shelly, S. Y. Schwartz, W. Rabbel, M. Thorwart, and H. Kao (2009), Deep low-frequency earthquakes in tremor localize to the plate interface in multiple subduction zones, *Geophys. Res. Lett.*, *36*, L19306, doi:10.1029/2009GL040027.

Ghosh, A., J. E. Vidale, J. R. Sweet, K. C. Creager, and A. G. Wech (2009a), Tremor patches at Cascadia revealed by array analysis, *Geophys. Res. Lett.*, *36*, L17316, doi:10.1029/2009GL039080.

Ghosh, A., J. E. Vidale, Z. Peng, K. C. Creager, and H. Houston (2009b), Complex nonvolcanic tremor near Parkfield, California, triggered by the great 2004 Sumatra earthquake, *J. Geophys. Res.*, *114*, B00A15, doi:10.1029/2008JB006062.

Ghosh, A., J. E. Vidale, J. R. Sweet, K. C. Creager, A. G. Wech, and H. Houston (2010), Tremor bands sweep Cascadia, *Geophys. Res. Lett.*, *37*, L08301, doi:10.1029/2009GL042301.

Hyndman, R. D., and S. M. Peacock (2003), Serpentinization of the forearc mantle, *Earth Planet. Sci. Lett.*, *212*(3–4), 417–432, doi:10.1016/S0012-821x(03)00263-2.

Kao, H., S. J. Shan, H. Dragert, G. Rogers, J. F. Cassidy, and K. Ramachandran (2005), A wide depth distribution of seismic tremors along the northern Cascadia margin, *Nature*, *436*(7052), 841–844, doi:10.1038/nature03903.

La Rocca, M., K. C. Creager, D. Galluzzo, S. Malone, J. E. Vidale, J. R. Sweet, and A. G. Wech (2009), Cascadia tremor located near plate interface constrained by S minus P wave times, *Science*, *323*(5914), 620–623, doi:10.1126/science.1167112.

Nadeau, R. M., and D. Dolenc (2005), Nonvolcanic tremors deep beneath the San Andreas Fault, *Science*, *307*(5708), 389, doi:10.1126/science.1107142.

Obara, K. (2002), Nonvolcanic deep tremor associated with subduction in southwest Japan, *Science*, *296*(5573), 1679–1681, doi:10.1126/science.1070378.

Peacock, S. M. (2009), Thermal and metamorphic environment of subduction zone episodic tremor and slip, *J. Geophys. Res.*, *114*, B00A07, doi:10.1029/2008JB005978.

Power, W. L., and T. E. Tullis (1992), The contact between opposing fault surfaces at Dixie Valley, Nevada, and implications for fault mechanics, *J. Geophys. Res.*, *97*(B11), 15,425–15,435, doi:10.1029/92JB01059.

Resor, P. G., and V. E. Meer (2009), Slip heterogeneity on a corrugated fault, *Earth Planet. Sci. Lett.*, *288*, 483–491, doi:10.1016/j.epsl.2009.10.010.

Rubin, A. M., D. Gillard, and J. L. Got (1999), Streaks of microearthquakes along creeping faults, *Nature*, *400*(6745), 635–641, doi:10.1038/23196.

Rubinstein, J. L., J. E. Vidale, J. Gomberg, P. Bodin, K. C. Creager, and S. D. Malone (2007), Non-volcanic tremor driven by large transient shear stresses, *Nature*, *448*(7153), 579–582, doi:10.1038/nature06017.

Sagy, A., E. E. Brodsky, and G. J. Axen (2007), Evolution of fault-surface roughness with slip, *Geology*, *35*(3), 283–286, doi:10.1130/G23235A.1.

Segall, P., and A. M. Bradley (2009), Numerical models of slow slip and dynamic rupture including dilatant stabilization and thermal pressurization, *Eos Trans. AGU*, *90*(52), Fall Meet. Suppl., Abstract T22B-08.

Shelly, D. R. (2009), Possible deep fault slip preceding the 2004 Parkfield earthquake, inferred from detailed observations of tectonic tremor, *Geophys. Res. Lett.*, *36*, L17318, doi:10.1029/2009GL039589.

Shelly, D. R., G. C. Beroza, S. Ide, and S. Nakamula (2006), Low-frequency earthquakes in Shikoku, Japan, and their relationship to episodic tremor and slip, *Nature*, *442*(7099), 188–191, doi:10.1038/nature04931.

Shelly, D. R., G. C. Beroza, and S. Ide (2007a), Complex evolution of transient slip derived from precise tremor locations in western Shikoku, Japan, *Geochem. Geophys. Geosyst.*, *8*, Q10014, doi:10.1029/2007GC001640.

Shelly, D. R., G. C. Beroza, and S. Ide (2007b), Non-volcanic tremor and low-frequency earthquake swarms, *Nature*, *446*(7133), 305–307, doi:10.1038/nature05666.

Shelly, D. R., W. L. Ellsworth, T. Ryberg, C. Haberland, G. S. Fuis, J. Murphy, R. M. Nadeau, and R. Burgmann (2009), Precise location of San Andreas Fault tremors near Cholame, California using seismometer clusters: Slip on the deep extension of the fault?, *Geophys. Res. Lett.*, *36*, L01303, doi:10.1029/2008GL036367.

Smith, R. B. (1975), Unified theory of onset of folding, boudinage, and mullion structure, *Geol. Soc. Am. Bull.*, *86*(11), 1601–1609, doi:10.1130/0016-7606(1975)86<1601:UTOTOO>2.0.CO;2.

Smith, R. B. (1977), Formation of folds, boudinage, and mullions in non-Newtonian materials, *Geol. Soc. Am. Bull.*, *88*(2), 312–320, doi:10.1130/0016-7606(1977)88<312:FOFBAM>2.0.CO;2.

Turcotte, D. L., and G. Schubert (2002), *Geodynamics*, 2nd ed., Cambridge Univ. Press, New York.

Wech, A. G., and K. C. Creager (2008), Automated detection and location of Cascadia tremor, *Geophys. Res. Lett.*, *35*, L20302, doi:10.1029/2008GL035458.

Wessel, P., and W. H. F. Smith (1998), New improved version of generic mapping tools released, *Eos Trans. AGU*, *79*(47), 579, doi:10.1029/98EO00426.